

ROVERD: USE OF TEST DATA IN GSI-191 RISK ASSESSMENT

Ernie Kee^{*a}, John Hasenbein^b, Alex Zolan^b, Phil Grissom^c, Seyed Reihani^g, Fatma Yilmaz^d, Bruce Letellier^e, Vera Moiseytseva^f, and David Imbaratto^h

^aTexas A&M University, College Station, TX, erniekee@tamu.edu

^bThe University of Texas at Austin, Austin, TX, jhas@mail.utexas.edu, alex.zolan@utexas.edu

^cSouthern Nuclear Company, Birmingham, AL, pdgrisso@southernco.com

^dSouth Texas Project NOC, Wadsworth, TX, fyilmaz@stpegs.com

^eAlion Science and Technology, Albuquerque, NM, bletellier@alionscience.com

^fYK.risk, LLC, Bay City, TX, vera.m76@gmail.com

^gThe University of Illinois at Urbana-Champaign, sreihani@illinois.edu

^hPG&E, Diablo Canyon Power Plant, dni3@pge.com

Abstract

An approach that would use test data to evaluate the risk associated with the concerns raised in GSI-191 is described. The relationship to the elements of quantitative risk-informed regulation for addressing the concerns raised in GSI-191 in PWR plant licensing is described. Use of experimental data from a deterministic sump performance test to establish scenario success for tested debris loads is summarized and compared to the licensing requirements in the regulations. Generation and transport of debris to ECCS sump from LOCA is described and data are shown for a particular PWR. Application of the analysis results to a license amendment for an operating PWR is summarized.

Acronyms

CASA Grande	Containment Accident Stochastic Analysis (CASA) Grande
CDF	Core Damage Frequency
ΔCDF	Change in core damage frequency above a baseline level
ΔLERF	Change in large early release frequency above a baseline level

*Corresponding author

CSS	Containment Spray System
DEGB	Double-Ended Guillotine Break
ECCS	Emergency Core Cooling System
FA	Fuel Assembly. Several fuel assemblies are loaded in the reactor vessel to form the reactor core
GDC	General Design Criteria (Appendix A to Part 50 of the code of federal regulations)
GSI-191	Generic Safety Issue 191 - the NRC Generic Safety Issue number 191
LAR	License Amendment Request
LDFG	Low Density Fiberglass (such as NUKON™)
LERF	Large Early Release Frequency
LLOCA	Large Break Loss of Coolant Accident
LOCA	Loss of Coolant Accident
NRC	The Nuclear Regulatory Commission
PRA	Probabilistic Risk Assessment
PWR	Pressurized Water Reactor
PWROG	Pressurized Water Reactor Owners Group
RCB	Reactor Containment Building
RCS	Reactor Coolant System
ROVERD	Risk-informed Over Deterministic
RWST	Refueling Water Storage Tank
SI	Safety Injection System
STP	South Texas Project

STPNOC	The STP Nuclear Operating Company
TSP	Trisodium phosphate ($\text{Na}_3\text{PO}_4 \cdot 12\text{H}_2\text{O}$) sump water pH buffer chemical
ZOI	Zone of Influence
D_i^{small}	corresponds to the smallest break size at any particular location that produces more fines in the ECCS sump than the tested amount

1 Introduction

GSI-191 is the long-standing NRC safety issue (see NRC, 2003, for example) related to effects of debris transported to PWR ECCS sumps following hypothesized LOCAs. Such debris may cause clogging of ECCS sump strainers intended to protect equipment in the system. Any debris passing through the inefficient sump strainers could furthermore cause blockage of the reactor core cooling channels resulting in overheating and subsequent failure of the fuel cladding.

ROVERD is a method intended to simplify risk assessment of the concerns raised in GSI-191 by dividing LOCA scenarios in two categories designated as ‘deterministic’ and ‘risk-informed’ (Figure 1). The deterministic scenarios are those in which the amount of LDFG fiber fines estimated to arrive in the ECCS sump is equal to, or less than, the amount used in an acceptable test¹ and require no further processing. Otherwise, scenarios are assigned to a ‘risk-informed’ category. When making a category determination, the amount of fines must include eroded fines and fines associated with tramp dust and dirt. Risk-informed scenarios are evaluated as illustrated in Figure 2 to obtain ΔCDF . As shown, the PRA is used to obtain the rest of the quantitative measures required by Regulatory Guide 1.174 (NRC, 2011), CDF, LERF and ΔLERF .

Although we make reference to Regulatory Guide 1.174, our focus is on quantification of the

¹As used in here, ‘acceptable’ means a plant-specific test designed to check sump strainer performance in the most limiting conditions utility investigators can determine. Normally, the test is reviewed by the NRC for use in licensing activities.

risk it requires. Defense-in-depth and safety margin, also required by Regulatory Guide 1.174 to successfully implement a risk-based solution are not addressed in here. Implementing ROVERD in a plant license amendment additionally requires examination of GDC and other plant license commitments which are beyond the scope of this article.

In ROVERD, ΔCDF is derived directly from LOCA frequencies based on break size diameters. Section 2 (LOCA frequencies), summarizes the ‘top down’ frequency method used for this purpose. Due to the novel approach used in ROVERD to evaluate ΔCDF , we provide a relatively detailed description. One of the requirements is adequate cooling flow as summarized in Section 3 (RCS Thermal-hydraulics). After recirculation switchover, the fiber mass accumulated in the RCB sump then flows to the core. Section 4 (Transport during recirculation) is a description of how the fiber is collected and transported in the analysis. Thermal-hydraulic analysis and fiber accumulation are used in analysis of in-core effects as summarized in Section 5, (Core performance metrics). Section 6 concludes the article.

2 LOCA frequencies

Although the ECCS strainer may operate under several different plant states, strainer tests are usually designed to represent plant states congruent with deterministic assumptions. In particular, strainer tests are designed to match equipment failure assumptions (from GDC) taken in the plant updated final safety analysis report on train availability (referred to as ‘plant states’).

Because many different plant states may need to be evaluated, and depending on details associated with the test used in the ROVERD deterministic assessment, additional analysis may be required to assess risk (generally, a bounding assessment) associated with plant states not tested. We include an example of such an analysis in the following.

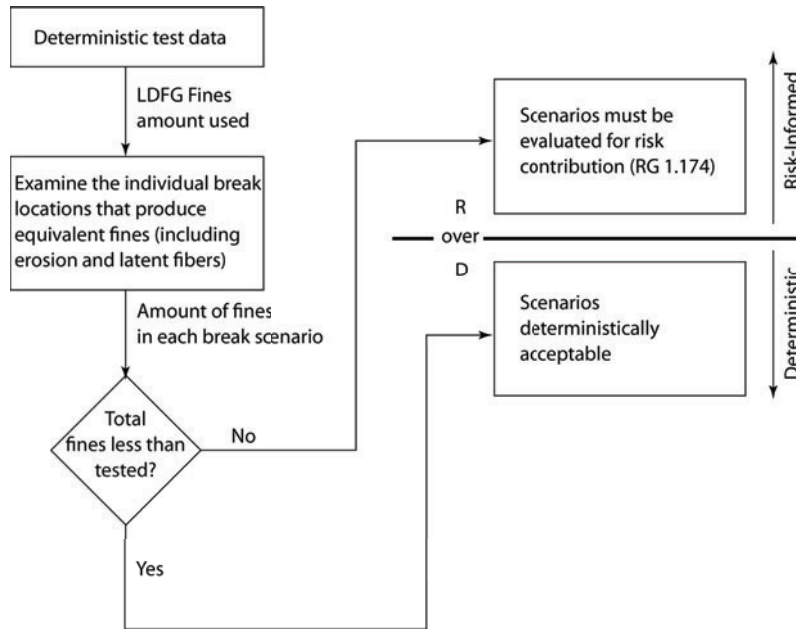


Figure 1: ROVERD separates those scenarios that go to success deterministically from those that are assumed to go to failure and require risk-informed analysis

2.1 Frequency determination

A fundamental goal of the RoverD approach is to determine the total frequency of breaks that fall into the risk-informed category. In a preprocessing step known as RoverD’s *fetch stage*, exhaustive break assessments (hundreds of thousands of LOCA scenarios) are performed in a computer application (Alion Science & Technology, 2015, for example) to identify all weld locations, with corresponding break sizes, which produce more than the allowable amount of fiber fines.

With fetch completed, ROVERD has data that can be thought of as ordered pairs consisting of a weld index and a break size. For now, assume that I weld locations are in the risk-informed category and these locations are indexed by $i = 1, \dots, I$. Each weld location i then has a corresponding break size D_i^{small} which caused it to be placed in the risk-informed category. It is possible that for a single weld, multiple break scenarios caused it to be put in this category. If so, define D_i^{small} to be the smallest such break size.

Now, recall that the goal is to determine the overall frequency of events that generate

too many fiber fines. First, for each weld i in the risk-informed category the goal is to determine the frequency of breaks that exceed D_i^{small} . This is called $F(D_i^{small})$ and is the frequency of unacceptable events caused by that particular weld. Then, the overall frequency of unacceptable events caused by breaks in the risk-informed category is simply the sum of these frequencies:

$$\Phi = \sum_{i=1}^I F(D_i^{small}).$$

In general, as shown in Figure 3, interpolation is required to obtain frequencies at break sizes, D_i^{small} , and pipe diameters other than values elicited by Tregoning et al. (2008). We have studied “naive” interpolation methods based on log and linear approaches. It can be shown that among three of these naive methods, linear-linear produces higher values Hasenbein (2015, linear-linear, log-linear, and log-log) and we adopted that method in ROVERD.

To explain the calculations, we first focus on Weld 5 from Figure 3, a particular weld in pipe of category 1, which is denoted by \mathbb{D}_1 . To de-

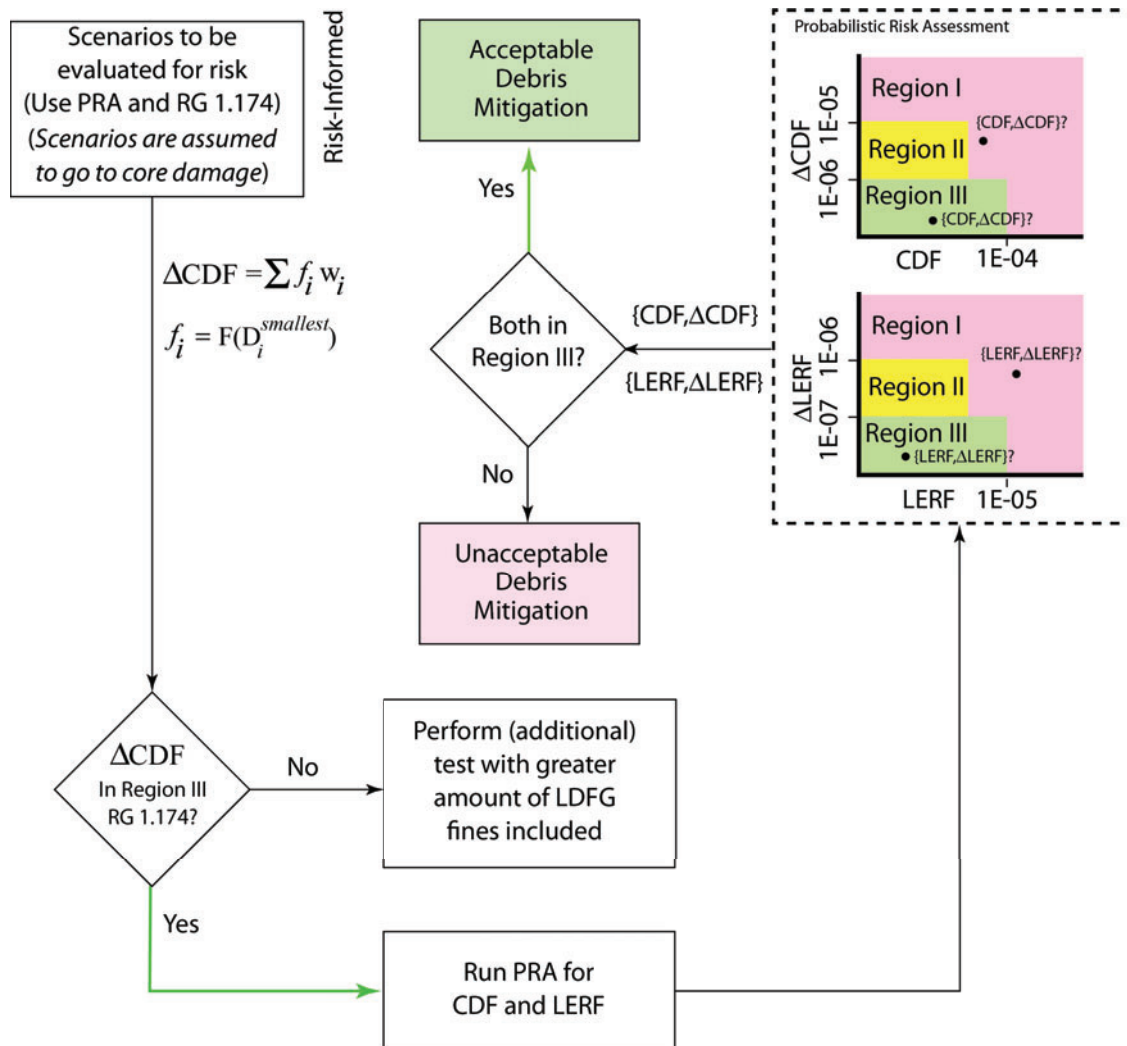


Figure 2: Flow chart showing the ROVERD evaluation process following categorization of scenarios to determine risk acceptability. In this depiction, the frequency, f_i , of break at any location is determined by the diameter as determined in NUREG 1829.

termine $F(D_5^{small})$, the goal is to be consistent with NUREG-1829. For now, the median values from Tregoning et al. (2008, Table 7.19) are used. Let $f(D_5^{small})$ be the exceedance frequency for a break of size D_5^{small} as implied by median values from Tregoning et al.

Plant-wide, the frequency of breaks of size D_5^{small} and larger is

$$f(D_5^{small}).$$

Shown along the bottom of Figure 3 are categories defined by increasing pipe sizes. We define

$Cat(D_i^{small})$ as $0 < \mathbb{D}_1 < \mathbb{D}_2 < \dots < \mathbb{D}_{j-1} < D_i^{small} < \mathbb{D}_j < \dots < \mathbb{D}_{n-1} < \mathbb{D}_n$, $Cat(D_i^{small}) = j$. Every weld that can experience a break of size D_5^{small} or larger contributes to the overall frequency. Hence, it is deduced that:

$$F(D_5^{small}) = \frac{f(D_5^{small})}{TW_1},$$

where TW_n for pipe size n is the total number of welds in pipes of this category or larger.

For a pipe in category 2, the calculation is similar. However, it should be noted that the de-

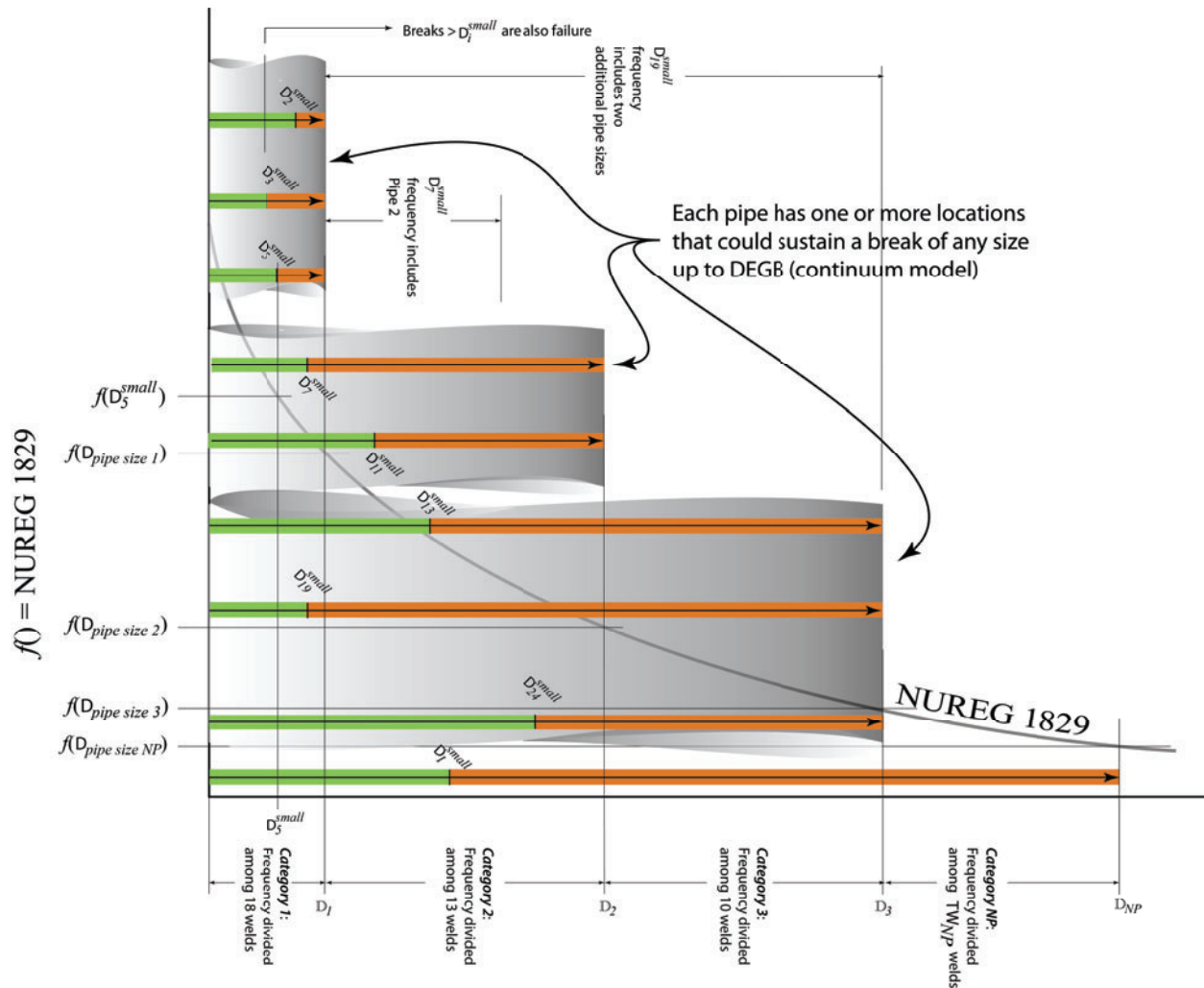


Figure 3: The top down approach assigns equally-weighted frequency in intervals between pipe diameter extents. Where D_i^{small} is in the interval, a second weighting is done to account for the success and failure portions.

nominator in the equation above depends only on the size of the break and not the category of pipe in which the weld resides. So, for Weld 7 in pipe category 2, D_7^{small} is smaller than D_1 . In this case, the frequency of a break of size D_7^{small} is

$$F(D_7^{small}) = \frac{f(D_7^{small})}{TW_1}.$$

For Weld 11, it is

$$F(D_{11}^{small}) = \frac{f(D_{11}^{small})}{TW_2}.$$

Now for any weld i in pipe category n with a

smallest break size D_i^{small} a general formula can be written:

$$F(D_i^{small}) = \frac{f(D_i^{small})}{TW_{Cat(D_i^{small})}}. \quad (1)$$

$Cat(D_i^{small})$ is the pipe category corresponding D_i^{small} . For example, if Category 1 is 1-inch pipes and category 2 is 2-inch pipes, then for a break of 1.75in, $Cat(1.75in) = 2$.

Now, let R_n be the set of all welds which are in the risk-informed category and are associated

with pipes of category n . Then, the frequency of unacceptable events due to weld breaks in pipes of category n can be written as:

$$\sum_{i \in R_n} F(D_i^{small}).$$

Finally, the overall frequency of events in the risk-informed category is given by:

$$\Phi = \sum_{n=1}^{NP} \sum_{i \in R_n}^I F(D_i^{small}). \quad (2)$$

2.2 Plant states not tested (STP)

Single ECCS/CSS train operation is not assumed in a deterministic STP LOCA evaluation and therefore is an untested configuration. However, in a risk-based assessment, single train operation is possible and for certain scenarios, single train operation is assessed to go to success in the PRA. In the STP ECCS design, single train operation could result in as much as twice the debris load on the operating strainer. Therefore in ROVERD, breaks that could be tolerated in single train operation are those with one half the tested debris load.

The break frequency description above would apply in the same way to the single train operation, but would clearly result in higher frequencies due to the increased debris load. To account for the increased risk, data elicited by Tregoning et al. (2008, Tables 7.11 and 7.19) could be assessed for the cases where two or three trains are operating (cases either tested or bounded by the test) and assessed again for the untested case (single train operation) with the higher frequency. For example, if f_2 is the success frequency for two or more trains operating and f_1 is the success frequency for single train operation, (2) can be rewritten to accommodate the total frequency, $\hat{\Phi}$, for both operating states:

$$w_j = \frac{f_j}{\sum_j f_j}; \quad j = 1, 2, \quad (3a)$$

$$\Phi_j = w_j \sum_{n=1}^{NP} \sum_{i \in R_n}^I F(D_i^{small}), \quad (3b)$$

$$\hat{\Phi} = \sum_j \Phi_j. \quad (3c)$$

2.3 Example of implementation (STP)

Application of the method for risk evaluation is summarized in the following. Two Cases (Case 1 and Case 2) other than the condition tested in (AREVA, 2008) represent bounding cases for fine fiber amounts. Case 1 is the most likely case (when all strainers are in operation). In this case, far less fiber will accumulate on each strainer than in the tested case. Therefore, Case 1 is bounded by the tested case.

However Case 2 corresponds to a case with less than the tested number of trains (beyond design basis) of the three strainers are in operation. Although the case is beyond design basis, it needs to be considered in the risk analysis since at least twice as much fiber would accumulate on the single strainer than when two or more strainers are in operation. In this case, only 1/2 the tested amount of fine fiber can be assumed to be tolerated. When all cases are considered using (3), a slightly higher Δ CDF is estimated.

Table 1 summarizes the Δ CDF estimate for geometric and arithmetic averages from Tregoning et al. (2008). The frequencies for the bounding cases are $f_2 = 3.32\text{E-}6\text{yr}^{-1}$ (Case 1) and $f_1 = 4.34\text{E-}8\text{yr}^{-1}$ (Case 2). As shown, the median Δ CDF is within Region III of the Regulatory Guide 1.174 evaluation ($\ll 1.0\text{E-}06$).

As shown in Table 1, only the 95th percentile of the arithmetic mean estimate exceeded the Region III criterion (NRC, 2011, Figures 4 and 5). As summarized by Morton et al. (2014), the geometric method of aggregation is the most appro-

Table 1: Case 1 and Case 2 results for geometric (GM) and arithmetic (AM) aggregations of Tregoning et al. (2008, Tables 7.11 and 7.19) data. Frequencies are in events/yr. Also shown are the results for a DEGB-only model for the locations that go to failure.

Continuum Break Model						
Quantile	Case 1 GM	Case 1 AM	Case 2 GM	Case 2 AM	$\hat{\Phi}$ (GM)	$\hat{\Phi}$ (AM)
5 th	2.54E-10	9.58E-09	2.58E-09	3.02E-08	2.84E-10	9.85E-09
50 th	7.20E-09	1.61E-07	5.83E-08	3.65E-07	7.86E-09	1.64E-07
95 th	3.29E-07	1.16E-06	1.29E-06	4.56E-06	3.41E-07	1.20E-06
Mean	1.12E-07	7.04E-07	3.39E-07	1.93E-06	1.15E-07	7.20E-07
DEGB-Only Model						
5 th	9.84E-11	9.03E-09	1.14E-09	2.27E-08	1.12E-10	9.21E-09
50 th	2.88E-09	2.07E-07	2.64E-08	3.90E-07	3.18E-09	2.09E-07
95 th	1.48E-07	1.14E-06	6.86E-07	3.15E-06	1.55E-07	1.17E-06
Mean	5.12E-08	5.90E-07	2.03E-07	1.46E-06	5.32E-08	6.01E-07

appropriate estimator of LOCA frequency from (Tregoning et al., 2008).

We investigated the frequencies that would result under a DEGB assumption. That is, we asked if any D_i^{small} immediately progressed to the full diameter, what frequencies would be obtained? The results for DEGB are included in Table 1. It is interesting to note that for the 50th quantile, the frequency for the DEGB case increases slightly from the continuum model.

2.4 Δ LERF discussion

NRC (2011, see Figures 4 and 5, Page 16) requires quantitative evaluation of both pairs (CDF, Δ CDF) and (LERF, Δ LERF). Therefore, the LERF and Δ LERF need to be evaluated along with CDF and Δ CDF. We estimate CDF and LERF using the plant average PRA. Δ CDF is found as described in Section 2.1 and quantification of Δ LERF is described in the following.

Containment failure may be independent from the sump status and in these cases, the concerns raised in GSI-191 would not result in new early containment failure modes. Contributors to large early containment failure modes that need to be considered may include the following:

1. Containment bypass paths (including interfacing system LOCAs, steam generator tube

rupture initiating events, and induced steam generator tube ruptures).

2. Containment isolation failures.
3. High pressure melt ejection phenomena.
4. Core debris impingement on containment.
5. Reactor vessel and containment venting.
6. In-vessel steam explosions leading to containment failures (alpha mode failures).
7. Hydrogen burns leading to early containment failure.

Another consideration is the break size range. Because plants have been modified with very large ECCS strainers designed to accommodate large debris volumes, GSI-191 phenomena is likely to be only applicable for LLOCA. As a consequence, the primary early containment failure modes applicable for GSI-191 phenomena are extremely unlikely.

To ensure GSI-191 specific scenarios are appropriately considered, a sensitivity calculation for LLOCAs can be performed in which sump recirculation is assumed failed by strainer plugging (all scenarios go to core damage). CDF and

LERF under this assumption can then be evaluated as follows (F implies ‘failed’):

$$\Delta LERF = \Delta CDF \left(\frac{LERF_{LLOCA, Sump=F}}{CDF_{LLOCA, Sump=F}} \right).$$

In a typical application, the fraction, $\frac{LERF_{LLOCA, Sump=F}}{CDF_{LLOCA, Sump=F}}$ is very small (on the order of 1.0E-03). As a consequence $\Delta LERF$ should not be a concern for most applications.

2.5 Summary

In summary, the risk-informed scenarios are assumed to result in core damage and contribute their frequency weight to ΔCDF . At any location where there exists a failure producing more LDFG fines than the amount tested (by AREVA, 2008, for example), the frequency associated with the smallest size break at that location, D_i^{small} , which produces more fines than the tested amount, is obtained from (2) or (3). (2) and (3) follow the “top down” strategy of Popova and Morton (2012) that preserves the frequencies (or frequency quantiles) developed by Tregoning et al. (2008).

3 RCS Thermal-hydraulics

During an hypothesized LOCA, flow discharged from the break may depressurize the RCS to the point SI is actuated and pumping equipment as well as passive systems are made available to supply water to the RCS. Depending on the LOCA size hypothesized, the SI may begin injecting water immediately into the cold leg injection point (see Figure 5) or after the operators start controlled cool down and depressurization.

Depending on the break location and size, in the hot leg or in the cold leg, more (or less) debris will collect in the core fuel assemblies. Breaks in the hot leg pull water up through the core. However, only the flow required to balance decay energy release, flows up into the core in a cold leg break, the rest flows out the break (see Figure 4 on page 9).

Initially, flow from the RWST is supplied free of the debris produced by the hypothesized LOCA. If the operators can’t cool down and depressurize the plant before the RWST empties, the ECCS is switched to the recirculation mode. In this mode, there is potential for debris that may pass through the ECCS sump screens to partially or fully block the core fuel channels and other paths, especially core bypass paths, through the reactor vessel.

Vaghetto and Hassan (2013) studied the behavior of the RCS for scenarios where the fuel channels and the core bypass flow paths were fully blocked. Based on fuel peak clad temperature, they showed that unless the LOCA was large and located on the cooling water return side (cold leg) of the RCS, debris blockage of the fuel for STP cores (for example) is not a concern for core cooling.

4 Transport during recirculation

NEI (2004) developed an acceptable methodology for determining the amount of debris generated in a LOCA of any particular size by defining a ZOI. Within the ZOI, specific size distributions of LDFG particles can be estimated using acceptable methods (Figure 4a).

The amount and speciation of debris transported to the ECCS sump can be estimated using logic trees that fractionate debris amounts captured and sequestered, and the amounts that would continue to transport (for example see NEI, 2004, ppg 3-45, 3-53). ROVERD uses a ‘worst case’ set of assumptions in development of the STP debris transport logic tree.

The flow paths through the RCB with the water flowing out of the breach in the RCS as well as with water from sources such as ECCS and CSS during the recirculation phase are shown in Figures 4b and 4c. CASA Grande performs mass conservation of debris species in the containment pool (M_p), on the ECCS strainers, (M_s) and in the reactor core, (M_c), (Figure 6).

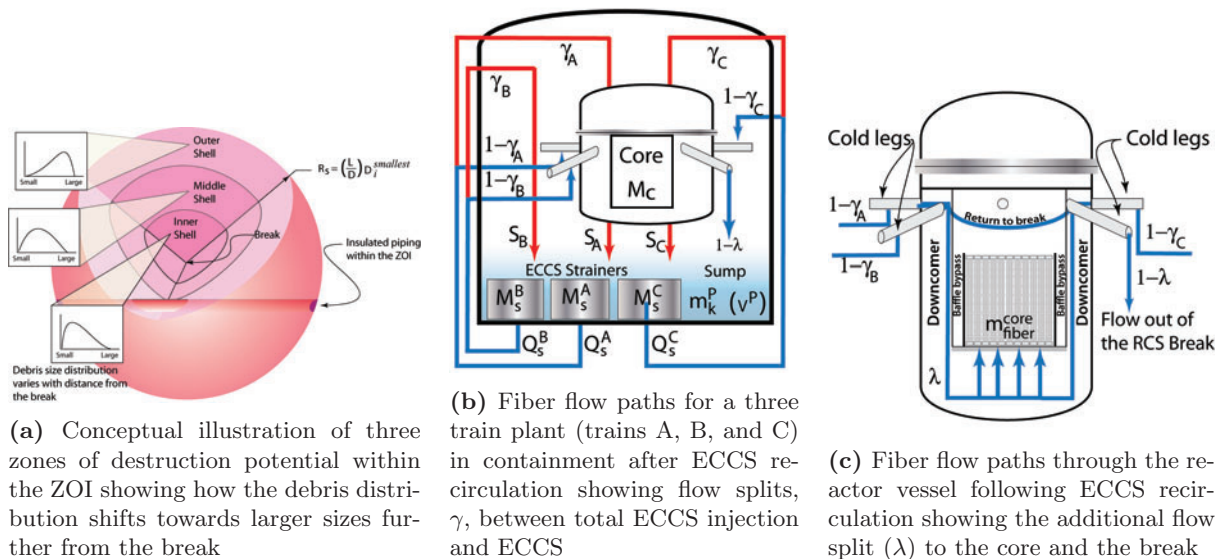


Figure 4: Flow paths through the containment and reactor vessel following the start of ECCS recirculation showing where fiber mass (m) is conserved (ECCS strainers, ECCS sump, and the reactor core)

Although different size particles are created from partially destroyed fiberglass insulation strands within the ZOI (Figure 4a), the smallest particles that transport readily through the RCB are ‘fines’. Larger and partially destroyed LDFG insulation either do not transport or quickly sink in the ECCS sump and remain there but over time, water flowing through the RCB tends to erode some of the larger particles captured outside of the ECCS sump into fine particles. Besides LDFG either destroyed or eroded into fine particles, fine particles from tramp dust and dirt need to be taken into account.

A break size and location define a scenario from which is derived the amount of LDFG fines that arrive in the ECCS sumps. The methodology for exhaustively examining hundreds of thousands of possible break sizes, orientations, truncation of ZOIs, transport of fines, and erosion of LDFG requires a computational framework implemented on a computer (Alion Science & Technology, 2015, for example).

A flow network that approximates the transport and capture of debris in containment is shown in Figure 6. The primitive data for this system are: 1) time-dependent flows $Q_s(\cdot)$ and

$Q_c(\cdot)$, 2) scalars V_p , $M_p(0)$, and γ . The flows are time-dependent due to the influence of Q_c on λ . Q_c as a function of time is obtained from a table and is governed by the decay heat level. Given these model primitives, an analysis of the time-dependent accumulation of debris on the strainer, core, and in the pool can be performed. These functions are governed by a set of non-linear differential equations. The non-linearity arises due to the *filtration function*, as shall become apparent in the sequel.

The transportable debris from the hypothesized LOCA moves down into the containment emergency sump forming a pool of water (Figure 5). The initial concentration of debris in the containment emergency sump water pool is $C_p(0) = \frac{M_p(0)}{V_p}$. At the start of the ECCS recirculation phase, we assume all the transportable debris is in the pool. Hence, there is none on the strainer or the core ($M_s(0) = 0$ and $M_c(0) = 0$). The rate of accumulation of the debris on the strainer and the core is governed by the amount that passes through the strainer as the flows transport it and by the amount deposited on the core. With respect to the flow equations below,

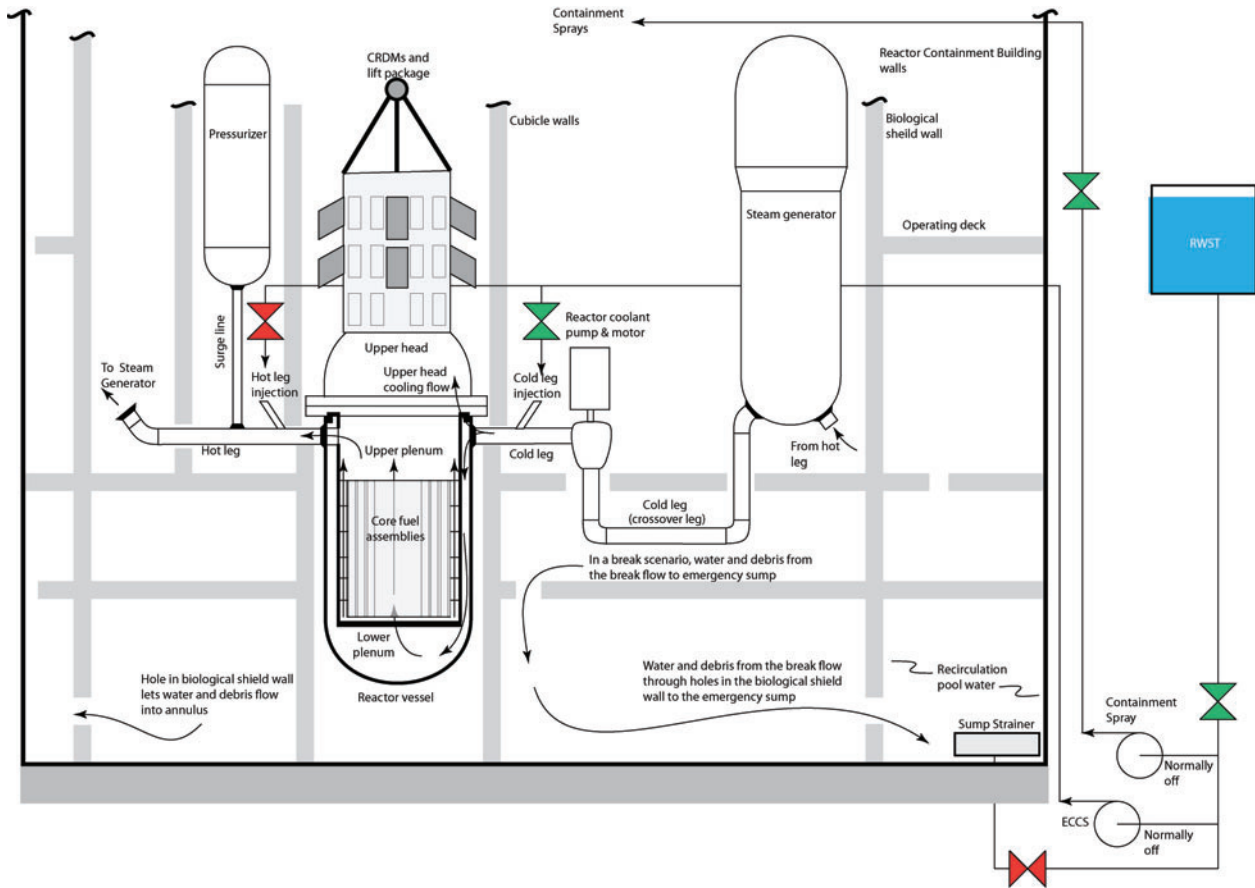


Figure 5: Simplified arrangement of the reactor system with flow directions shown during normal operation. The arrangement has been distorted so the flows and equipment can be seen.

the core acts as a sink. The governing conservation equations are:

$$\frac{d}{dt} M_s^k(t) = Q_s^k(t) C_p(t) f(M_s^k(t)), \quad (4)$$

$$\frac{d}{dt} M_c(t) = Q_c(t) C_p(t) \frac{\sum_k [(1 - f(M_s^k)) (1 - \gamma^k) Q_s^k(t)]}{\sum_k [(1 - \gamma^k) Q_s^k(t)]} \quad (5)$$

$$0 = \frac{d}{dt} M_p(t) + \frac{d}{dt} \sum_k M_s^k(t) + \frac{d}{dt} M_c(t), \quad (6)$$

where k is the strainer index. Wherever k appears the index is taken over all the values in $\{A, B, C\}$, i.e., the three strainers. The initial conditions and boundary conditions are:

$f(M_s)$ is a fraction between 0 and 1, dependent on the amount of mass on the strainer (Ogden et al., 2013, Figure 13),

$Q_s(\cdot)$ should be treated generally as a function of time to model pumps turning on and off (discrete tabular function),

$Q_c(\cdot)$ is a known function of time (discrete tabular function),

V_p is a given constant value,

The initial mass on the core is $M_c(0) = 0$,

The initial mass in the pool, $M_p(0)$, is given,

And $C_p(t) = M_p(t)/V_p$.

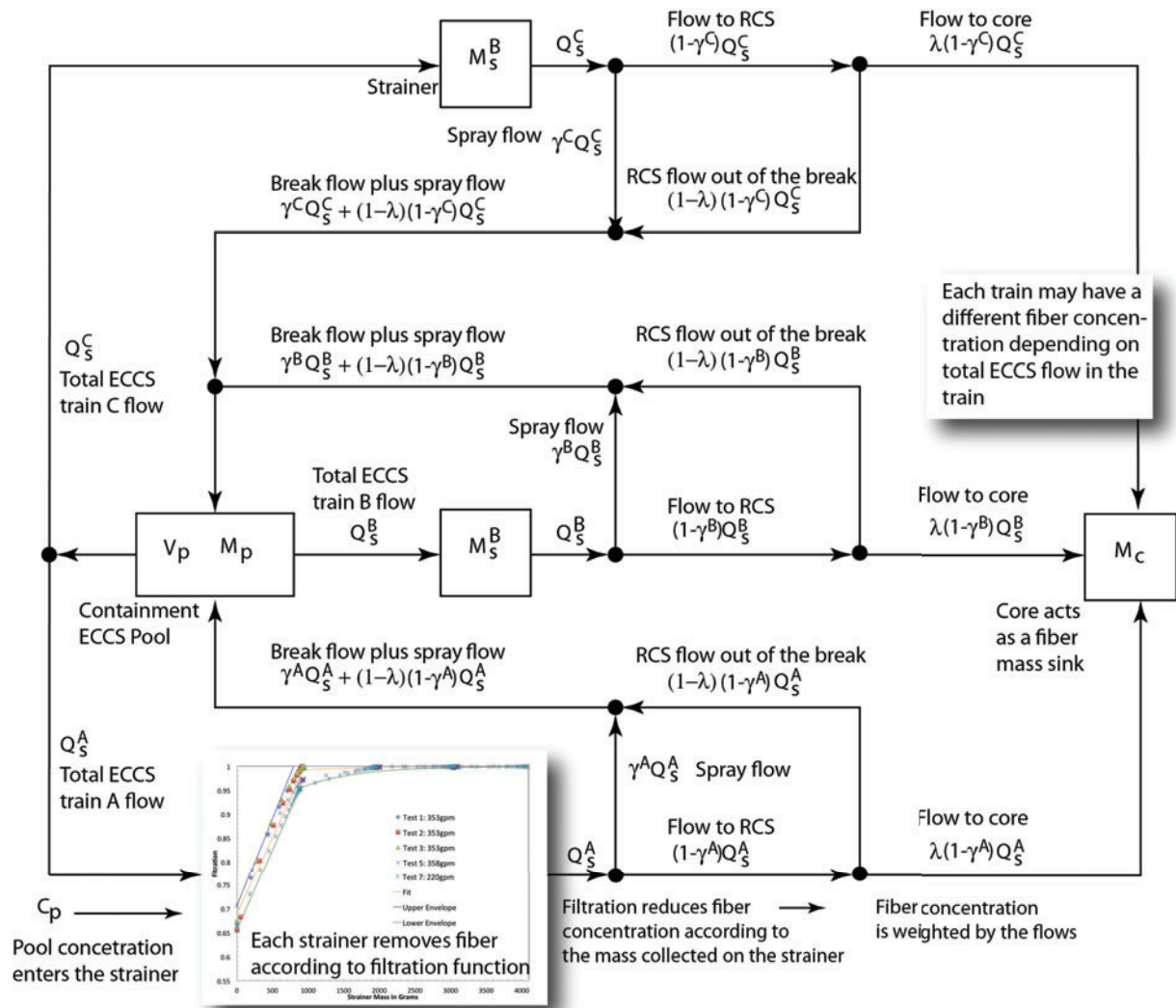


Figure 6: Flow network for one of three trains showing the three places debris is caught: the pool, the strainer, and the core. Shown as well are the various flow splits that take place between the places debris is caught. The flow split λ is defined by the amount of flow demanded by the core to remove decay heat.

4.1 Implementation

(4) to (6) were integrated in a Python implementation for a PWR to investigate the effectiveness of the ECCS strainers for core fiber accumulation during a cold leg break scenario. The integration was performed for extreme cases of ECCS sump pool LDFG fiber concentrations and envelopes (low and high) for the PWR ECCS filters' filtration fit shown in Figure 7 (Ogden et al., 2013).

Results of integration over 50 minutes (when

steady state was reached) for bounding cases of initial pool concentration and filtration efficiency envelopes are shown in Figure 8. As can be seen in the results, the most important parameter for the amount of fiber that arrives on the core (not surprisingly) is the ECCS filtration efficiency. Of course, the core flow rate is important, but it is fixed by the heat load required to remove decay heat, a well-established value. Other parameters (Q_s^k and γ^k) are less important.

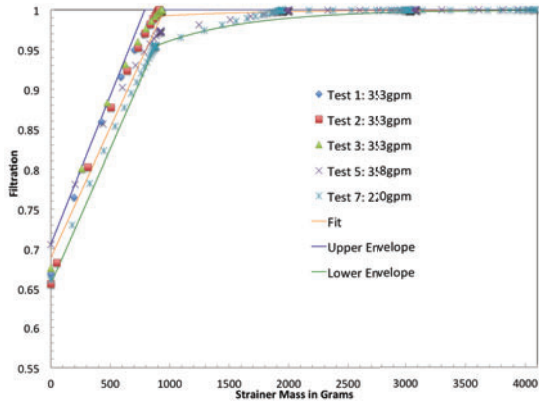


Figure 7: Filtration efficiency fits as a function of mass compared to measured data for the STP ECCS strainer modules. Efficiency fits obtained for the upper, central, and lower limits of the measurements are compared to the measured data.

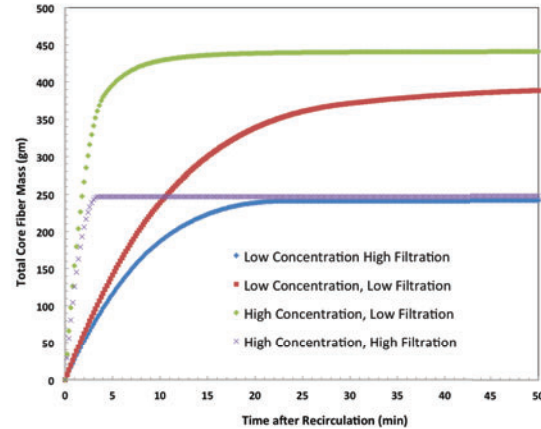


Figure 8: Comparison of bounding cases for core LDFG accumulation after start of ECCS recirculation. The mass accumulation should be divided by 193 to obtain gm/FA.

Table 2: Core mass accumulation for bounding cases of initial ECCS sump pool fiber concentration $C_p(t=0)$ and upper and lower bounds of filter efficiency.

Conc. gm/GAL	lower (gm)	upper (gm)
High (0.832)	441	247
Low (0.158)	400	241

5 Core performance metrics

In addition to satisfying the strainer performance metrics, certain core performance must be acceptable with the amount of LDFG fines tested as well. There are two metrics, separately evaluated but ultimately having the same consequence, that must be found acceptable to categorize a scenario as deterministic. Decay heat removal considering LDFG blockage of the core cooling channels and freedom from boric acid precipitation must be found acceptable.

As described previously, Ogden et al. (2013) have shown that the amount of fiber penetrating through the ECCS sump screen is a function of ECCS LDFG loading. In order for the screen performance metrics as tested (again AREVA, 2008, for example) to serve as the

‘worst case’ condition for deterministic characterization, the amount of fiber passing through the ECCS strainers needs to be less than that tested by the PWROG as acceptable. The currently accepted allowable amount of fiber accumulation is 15 grams of fiber per FA (PWROG, 2011).

In addition to heat removal, the reactor core must remain below the precipitation limit for boric acid during the first few hours of the hypothesized LOCA. As a consequence of the presence of LDFG fiber transported to the fuel assemblies, boric acid buildup may be more than with the fuel assemblies clear of obstructions. Boric acid precipitation is a second core performance metric that must be evaluated as acceptable with the fraction of the tested amount of LDFG fibers passing through the ECCS strainers to the core (Section 4).

If the test design doesn’t match simulation, further testing could be designed based on lessons learned to converge on an acceptable result. If the test demonstrates acceptable ECCS and core performance metrics for the deterministic classifications and the risk is acceptable, then the risk margin obtained would provide a measure of the margin to the concerns raised in GSI-191 for the particular plant.

5.1 Plant assessments

ROVERD has been preliminarily applied to two four loop PWRs (Plant 1 and Plant 2) with existing acceptable tests. In Plant 1, there were 45 locations identified using with D_i^{small} (45 locations in the risk-informed category) that produced more than the tested amount of fiber fines in the sump. The risk-informed D_i^{small} ranged in size from 12.814 inches to 25.33 inches. Both of these PWRs use systems that help ensure containment integrity that are independent from the concerns raised in GSI-191.

Tregoning et al. (2008, Table 7.19) give quantiles derived using a geometric average of experts' inputs. Tregoning et al. also aggregated the expert's inputs using an arithmetic average (Tregoning et al., 2008, Table 7.11). The arithmetic aggregation of the experts' values are about an order of magnitude higher than the values aggregated using a geometric average. Insight to the potential range of results can be aided by evaluating the the methods used to aggregate experts' inputs.

Table 3 tabulates Δ CDF obtained at the quantiles published by Tregoning et al. for geometric and arithmetic aggregation. Plant 2 had D_i^{small} values that ranged from 27.5 in to 31 in. Because the exceedence frequencies drop off very quickly with break size, the smallest break diameter tends to drive the results.

6 Conclusions

A procedure has been described that would help utility investigators bound (in a local sense) the risk from concerns raised in GSI-191. The procedure would apply to LARs using a risk-informed approach structured around the recommendations made in Regulatory Guide 1.174. An overview of an implementation the procedure has been summarized.

Application using typical bounding test results has been shown for PWRs in which the concerns raised in GSI-191 apply. In both of these PWRs, the method would provide the necessary assurance that quantitative measures required

Table 3: Example evaluation of Δ CDF for two four loop PWR plants using LDFG insulation and TSP that have performed deterministic ECCS tests

Geometric Mean Aggregation		
	Frequency events/yr	
Quantile	Plant 1	Plant 2
5 th	2.54e-10	4.17e-11
50 th	7.2e-09	1.38e-09
95 th	3.29e-07	8.69e-08
Mean	1.12e-07	3.09e-08

Arithmetic Mean Aggregation		
	Frequency events/yr	
Quantile	Plant 1	Plant 2
5 th	9.58e-09	5.9e-09
50 th	1.61e-07	1.4e-07
95 th	1.16e-06	7.41e-07
Mean	7.04e-07	3.86e-07

by Regulatory Guide 1.174.

Reasonable methods to interpolate data developed by Tregoning et al. have been described and compared to actual results using software (CASA Grande) output data from a three ECCS train PWR plant simulation. ROVERD would help resolve uncertainty and bound risk in investigation of the concerns raised in GSI-191.

Acknowledgements

Alion Science & Technology work is funded by STPNOC contract BO4461, Revision 5. Reduction of CASA Grande results was performed at the University of Texas at Austin (UT Austin) by Jeremy Tejada under the direction of John Hasenbein and funded by STPNOC grant BO4425. The top down frequency methodology was developed by Elmira Popova at UT Austin, under STPNOC grant BO4425, Revision 0. Development of the strainer mass conservation equations was supported by Alex Zolan at UT Austin under the direction of John Hasenbein and funded by STPNOC grant BO4425, Revi-

sion 4. Seyed Reihani contributed to developing the mass conservation equations at the University of Illinois at Urbana Champaign under STPNOC grant BO5270, Revision 3. Implementation was ROVERD was supported by David Johnson and Don Wakefield at ABS Consulting under STPNOC contract BO5760, Revision 1 under STPNOC contract BO4461, Revision 6. Ernie Kee is funded by STPNOC under YK.risk, LLC contract BO5657, Revision 0 and Revision 1.

References

- Alion Science & Technology (2015, April). CASA Grande Theory Manual. ALION-SPP ALION-I009-10, Alion Science & Technology, Albuquerque, NM.
- AREVA (2008, August). South Texas Project Test Report for ECCS Strainer Testing. AREVA NP Document 66-9088089-000, AREVA NP, 7207 IBM Drive, Charlotte, NC 28262.
- Hasenbein, J. (2015, May). Order Relations for Concave Interpolation Methods. Technical Report 2015-001, The University of Texas at Austin, Austin, TX.
- Hasenbein, J., D. Morton, and J. Tejada (2014, May). RAI APLA-III-2: Modeling LOCA Frequency and Break Size under DEGB-only Breaks. STP_RIGSI191 RAI-APLA-III-2, The University of Texas at Austin, Austin, TX.
- Morton, D., Y. Pan, and J. Tejada (2014, April). Means of Aggregation and NUREG-1829: Geometric and Arithmetic Means. STP_RIGSI191 ARAI.01, The University of Texas at Austin, Austin, TX.
- NEI (2004, May). Pressurized Water Reactor Sump Performance Evaluation Methodology. Technical Report 04-07, Nuclear Energy Institute, 1776 I Street, Washington, DC.
- NRC (2003, February). Knowledge Base for the Effect of Debris on Pressurized Water Reactor Emergency Core Cooling Sump Performance. NUREG/CR 6808, Nuclear Regulatory Commission, Washington, DC.
- NRC (2011). Regulatory Guide 1.174: An Approach for Using Probabilistic Risk Assessment In Risk-Informed Decisions On Plant-Specific Changes to the Licensing Basis, Revision 2, Nuclear Regulatory Commission, Washington, DC.
- Ogden, N., D. Morton, and J. Tejada (2013, June). South Texas Project Risk-Informed GSI-191 Evaluation: Filtration as a Function of Debris Mass on the Strainer: Fitting a Parametric Physics-Based Model. Technical report, STP-RIGSI191-V03.06, The University of Texas at Austin, Austin, TX.
- Popova, E. and D. Morton (2012, May). Uncertainty modeling of LOCA frequencies and break size distributions for the STP GSI-191 resolution. Technical report, The University of Texas at Austin, Austin, TX.
- PWROG (2011, October). Evaluation of Long - Term Cooling Considering Particulate, Fibrous and Chemical Debris in the Recirculating Fluid. WCAP 16793, Pressurized Water Reactor Owners Group, Pittsburgh, PA.
- Tregoning, R., L. Abramson, and P. Scott (2008, April). Estimating Loss-of-Coolant Accident (LOCA) Frequencies Through the Elicitation Process. NUREG/CR 1829, Nuclear Regulatory Commission, Washington, DC.
- Vaghetto, R. and Y. A. Hassan (2013). Study of debris-generated core blockage scenarios during loss of coolant accidents using RELAP5-3D. *Nuclear Engineering and Design* 261(0), 144 – 155.